Talanta 83 (2010) 436–440

Contents lists available at ScienceDirect

Talanta

journal homepage: www.elsevier.com/locate/talanta

A study on lowering the detection limit with solid-state lead-selective electrodes

Grzegorz Lisak[a,b], Tomasz Sokalski[a], Johan Bobacka[a], Leo Harju[a], Andrzej Lewenstam[a,c,*]

[a] Laboratory of Analytical Chemistry and Centre for Process Analytical Chemistry and Sensor Technology 'ProSens', Process Chemistry Centre, Åbo Akademi University, Biskopsgatan 8, 20500 Åbo, Finland
[b] Graduate School of Chemical Sensors and Microanalytical Systems (CHEMSEM), Espoo, Finland
[c] AGH – University of Science and Technology, Faculty of Material Science and Ceramics, Mickiewicza 30, 30-059 Cracow, Poland

ARTICLE INFO

Article history:
Received 14 July 2010
Received in revised form
18 September 2010
Accepted 25 September 2010
Available online 1 October 2010

Keywords:
Low detection limit
Solid-state lead-selective electrode
Direct determination of lead

ABSTRACT

The detection limit of a Pb^{2+} ion-selective electrode with a solid state (PbS/Ag_2S) membrane was successfully lowered to the nanomolar range. The electrode was applied in direct potentiometric determination of Pb^{2+} in aqueous solutions. Hydrodynamics, redox reaction at the solid-state surface as well as time dependency were investigated and found as key factors affecting the low detection limit. By optimizing these parameters improving detection limit by ca. three orders of magnitude was achieved.

1. Introduction

The specific response of every ion selective electrode (ISE) to the analyte ion is limited by constitutive parameters of all ion-selective electrodes selectivity and detection limit [1]. Detection limit has been an issue of interest since early stages in the history of ISEs and initially solid-state membranes were in focus [2–4]. The possibility of lowering the detection limit for ISEs with plastic membranes was reported later. It initiated an intensive and interesting research focused exclusively on plastic membranes [1,5,6].

As shown recently successful application of this class of ISEs calls for in-depth understanding of the signal formation, dictated mainly by trans-membrane fluxes, and resulting optimization procedure. This fact encourages us to step back and to explore seemingly simpler membrane systems that are realized in case of ISEs with solid-state membranes. For these membranes the detection limit is primarily dictated by the solubility product of a sparingly soluble salt, often a single component of the membrane [3,4,7–11] and the thermodynamic unconditional solubility of the salts used offers a promise of low detection limit (see Table 1). It was suggested that by use of solid-state electrodes the detection limit could be even as low as 10^{-20} M [12].

Indeed, low detection limit dictated by thermodynamic solubility product was observed for numerous solid-state membrane ISEs. In purposely supported systems, i.e. in ionic buffers and in titrations, the free main ion activity and the solubility of solid-state membrane are purposely controlled by complexation and/or solubility reactions. This facilitates increasing the measurement range which is limited by known for these systems conditional solubility product [13]. In direct measurements with unbuffered samples or in unsupported calibrants conditional solubility as well governs the detection limit. However, the uncontrolled side reactions (e.g. protonation and complexation) and parasitic processes (e.g. oxidative membrane dissolution or adsorption on the membrane surface) effect the free main ion concentration and the membrane solubility in unfavorable and analytically difficult to control way. Typically, detection limits higher than that dictated by thermodynamic solubility products are observed [14]. In addition to the factors influencing solubility product, the bias from interfering ions, uncontrolled interference from supporting electrolyte, the adsorption of primary ions on the wall of the measuring containers, or non-controlled impurities could significantly affect the low detection limit [4,15]. For all above reasons the detection limit of a solid-state membrane ISE in direct unsupported measurement is typically not lower than 10^{-6} mol dm^{-3}. However, when side reactions and parasitic processes (including interference from other ions) are marginalized, the detection limit is improved to the one dictated by thermodynamic solubility product. In consequence, the Nernstian response of the electrode may be extended to the picomolar range. This has been convincingly documented in numerous papers [3,15–17]. Additionally, it was shown that in unbuffered

---

[*] Corresponding author at: Laboratory of Analytical Chemistry and Centre for Process Analytical Chemistry and Sensor Technology 'ProSens', Process Chemistry Centre, Åbo Akademi University, Biskopsgatan 8, 20500 Åbo, Finland.

E-mail addresses: andrzej.lewenstam@abo.fi, alewenst@abo.fi (A. Lewenstam).

0039-9140/$ – see front matter © 2010 Elsevier B.V. All rights reserved.
doi:10.1016/j.talanta.2010.09.043

Table 1
Solubility products and solubilities of the solid-state membrane components without considering side reactions [32].

Component of the solid-state membrane	$-\log K\mathrm{so}_{\mathrm{M}n\mathrm{S}}$	Solubility ($-\log S$) of M_nS
PbS	26.6	13.3
Ag_2S	49.2	16.6

media such ions as fluoride, chloride, iodide and sulfide can be readily measured down to 10^{-7} mol dm^{-3} [4,18–22].

Another practical aspect of concern in measurements in ultralow concentration ranges is the response time. As in the case of the ISEs with plastic membranes the equilibration processes can last for hours [4,23–25]. However, the length of that period should not discriminate the ISE from practical applications if the intention is to measure low concentrations.

The aim of this study is to re-examine the possibility of applying solid-state membrane electrodes for direct measurements of low concentrations of the main ion. A lead (II) ion-selective electrode is used and its performance at low concentrations of Pb^{2+} ions is inspected by different methods to establish a practical protocol for lowering detection limit.

2. Experimental section

2.1. Reagents

Lead (II) nitrate ($Pb(NO_3)_2$) and Tiron (4,5-dihydroxybenzene-1,3-disulphonic acid) were obtained from Fluka (Buchs, Switzerland). Potassium nitrate (KNO_3) was obtained from Merck (Darmstadt, Germany). Nitric acid (HNO_3), 65% was purchased from Baker (Deventer, the Netherlands). Sodium sulfide nonahydrate ($9H_2O{\cdot}Na_2S$) was purchased from Aldrich Chemical Company (Milwaukee, WI, USA). Trizma base (Tris[hydroxymethyl]aminomethane) for preparation of tris buffer was obtained from Sigma Chemical (Steinheim, Germany). The chemicals were of analytical grade. Aqueous solutions were prepared with freshly deionized water (18.2 MΩ cm) obtained with the ELGA purelab ultra water system (High Wycombe, United Kingdom).

2.2. EMF measurements

Two solid-state Pb^{2+}-ISEs (3:7 mol/mol PbS/Ag_2S) electrodes obtained from Volta (St. Petersburg, Russia) were used. A double-junction electrode Orion (Thermo Scientific-Environmental Instruments, Beverly, MA, USA) with 10^{-3} mol dm^{-3} KNO_3|1 mol dm^{-3} KCl served as a reference electrode. Potentiometric measurements were carried out in 100 ml disposable polystyrene beakers. Each beaker was soaked in 10^{-1} mol dm^{-3} HNO_3 for two days and was washed with deionized water before the measurement. Every day a pretreatment of the working and the reference electrodes was performed. The working electrodes were polished using 0.03 μm grain size Al_2O_3 powder while the inner compartment of the reference electrode was washed with 10^{-1} mol dm^{-3} HNO_3, deionized water and 10^{-3} mol dm^{-3} KNO_3, respectively. The obtained data was recorded with an EMF16 Interface from Lawson Labs Inc. (Malvern, PA, USA). All experiments were performed at room temperature (20–21 °C). The activity coefficients were calculated according to the Debye–Hückel approximation. All the EMF data were corrected for liquid-junction potentials according to the Henderson equation. Three methods (metal titration, standard calibration, kinetic calibration) were used to study the performance of Pb^{2+}-ISE at low concentrations of the analyte ion.

2.3. Metal titration

Metal titration was performed by addition of 10^{-3} mol dm^{-3} Tiron solution to the stock solution of 50 ml 10^{-5} mol dm^{-3} $Pb(NO_3)_2$ in Tris buffer, pH 8 adjusted by addition of concentrated nitric acid. The additions of the titrating agent were adjusted in such a way that the changes in free lead activity would be approximately half an order of magnitude. The pH was recorded using a combined glass electrode (Metrohm, Herisau, Switzerland). Free Pb^{2+} activities were calculated in the MathCAD program, MathSoft Engineering & Education, Inc. (Needham, MA, USA) based on Tiron concentration and pH values.

2.4. Standard calibration

Calibration of Pb^{2+}-ISE was done by automatic dilution of unbuffered lead (II) nitrate stock solution using two Metrohm Dosino 700 instruments equipped with burets of 50 ml capacity (Metrohm, Herisau, Switzerland). The pumps were programmed to dilute the sample solution with freshly deionized water (18.2 MΩ cm) every 30 min. Three different approaches were investigated (i) purging argon through the sample solutions, (ii) stirring, and (iii) purging with argon while stirring the sample solutions.

2.5. Kinetic calibration

Prior to calibration of the Pb^{2+}-ISE, the electrode was mechanically cleaned, as described above, and immersed for 300 s in the solution of 10^{-4} mol dm^{-3} Pb^{2+} to stabilize the readout. Then ionized lead was titrated with disodium sulfide to get 10^{-4} mol dm^{-3} S^{2-} and corresponding activity of lead ion, $a_{Pb^{2+}} \sim 10^{-15}$ mol dm^{-3}. The electrode was kept in this solution for 1000 s. Subsequently, the Pb-ISE and the reference electrodes were washed with deionized water, immersed in 50 ml of the sample solution and the kinetic curve was recorded. The sample solution was continuously stirred with a magnetic stirrer at an approximate speed of 1000 rpm. The potential was sampled every 60 s for about 11 000 s. Potential values were taken from the range 8000–10 000 s and an average value was used for preparing the calibration curve. Measurements were performed in the sequence of increasing lead activity in the sample solution starting from the solution of 10^{-10} mol dm^{-3} Pb^{2+}. The procedure was repeated three times for each activity, the standard deviation was calculated and included in the calibration curve. Perkin Elmer-Sciex Elan 6100 DRC Plus inductively coupled plasma mass spectrometry (ICP-MS) was used to control lead concentration in most diluted samples during kinetic calibration. In calculations of conditional solubility constant the data presented in [26] were used. The E–pH diagram was prepared by taking into account half reactions of reductions and oxidation of lead sulfide (PbS) in the water at a 25 °C. Standard potentials were calculated using the values of free Gibbs energies of each component [27].

3. Theoretical considerations

3.1. Selecting optimal conditions for measurements of low concentrations with solid-state Pb^{2+}-ISE

The space of parameters needed to be considered when solid-state ISE is used at concentrations close to the detection limit and in absence of interfering ions is depicted by the following semiempirical equation valid for solid-state membrane ISEs [4,28].

$$E = E^0 + \frac{RT}{z_I F} \times \ln \frac{1}{2}\left\{(a_I^A + \beta - \alpha + \gamma) + \left[(a_I^A + \beta - \alpha + \gamma)^2 + 4K'\right]^{1/2}\right\} \qquad (1)$$

where free main ion analytical activity (a_I^A), activity of the main ion due to oxidation (β) and reduction (α) of the solid-state membrane, the processes which liberate and consume the main ion respectively, surface activity of the main ion due to adsorption at the electrode membrane surface (γ), and K' is the conditional solubility product of sparingly soluble membrane salt; z_I the charge of the main ion, T is temperature in K; R, F gas and Faraday constants.

In the absence of redox and adsorption effects (α, β, $\gamma = 0$), the detection limit is governed exclusively by the conditional solubility product, K'. If solubility is increased by side reactions the actual solubility should be calculated from the conditional solubility product as shown below. The redox and adsorption processes, if present, would additionally contribute to the detection limit, because (α, β, $\gamma \neq 0$), see [4].

It was expected, and observed before, that the adsorption of the main ion, γ, is concentration (a_I^A) and time dependent, and so is the potential of the solid-membrane ISE, if adsorption predominates [4]. Resulting from this fact is the main idea in this study to cleanse the membrane properly thus assuring the reproducible renewal of the electroactive surface, and to take advantage of a reproducible adsorption [29]. This is a prerequisite for analytical usage of concentration dependent adsorption which paired with sufficiently low solubility could serve the effect of lowering the detection limit as shown below. The main challenge in such a case would be to select the optimal readout time. Such an optimized method in which both side reactions, redox effects are minimized and proper readout time selected is called here a kinetic method which will be discussed later.

3.2. Optimizing operating conditions for PbS-based ISE-theory

The following equation is valid for the conditional solubility product, K'_{PbS} of lead sulfide:

$$K'_{\mathrm{PbS}} = K_{\mathrm{PbS}}\alpha_{\mathrm{Pb(OH,X)}}\alpha_{\mathrm{S(H)}} \tag{2}$$

where K_{PbS} is thermodynamic (unconditional) solubility product of the reaction:

$$\mathrm{PbS} \rightleftharpoons \mathrm{Pb}^{2+} + \mathrm{S}^{2-} \tag{3}$$

while $\alpha_{\mathrm{Pb(OH,X)}}$ and $\alpha_{\mathrm{S(H)}}$ are side reaction coefficients, which depend on the extend of complex formation processes.

Without considering side-reactions $\alpha_{\mathrm{Pb(OH,X)}} = \alpha_{\mathrm{S(H)}} = 1$ and the activity of lead ions resulting from membrane dissolution is

$$[\mathrm{Pb}^{2+}] = \sqrt{K_{\mathrm{PbS}}} \sim 10^{-13.3} \tag{4}$$

Due to side-reactions of lead ions, i.e. complex formation with X^- and/or OH^- ions, and sulfide ions, i.e. protonation of S^{2-}, side reaction coefficients in the system are greater than one; $\alpha_{\mathrm{Pb(OH,X)}}$ and $\alpha_{\mathrm{S(H)}} > 1$. For such a case the conditional solubility product, K'_{PbS} is used for the calculation of the real solubility of PbS according to Ringbom [30]:

$$\alpha_{\mathrm{Pb(OH,X)}} = 1 + [\mathrm{OH}^-]K_{\mathrm{Pb(OH)}} + [\mathrm{OH}^-]^2K_{\mathrm{Pb(OH)_2}} + [\mathrm{X}^-]K_{\mathrm{Pb(X)}} + [\mathrm{X}^-]^2K_{\mathrm{Pb(X)_2}} \tag{5a}$$

$$\alpha_{\mathrm{S(H)}} = 1 + [\mathrm{H}^+]K_{\mathrm{HS}} + [\mathrm{H}^+]^2K_{\mathrm{H_2S}} \tag{5b}$$

where K are respective stability constants for indexed species.

The conditional solubility product allows calculating free lead ion activity due to membrane dissolution by the following equation:

$$[\mathrm{Pb}^{2+}] = \sqrt{K'_{\mathrm{PbS}}} = \sqrt{\frac{K_{\mathrm{PbS}}\,\alpha_{\mathrm{S(H)}}}{\alpha_{\mathrm{Pb(OH,X)}}}} \tag{6}$$

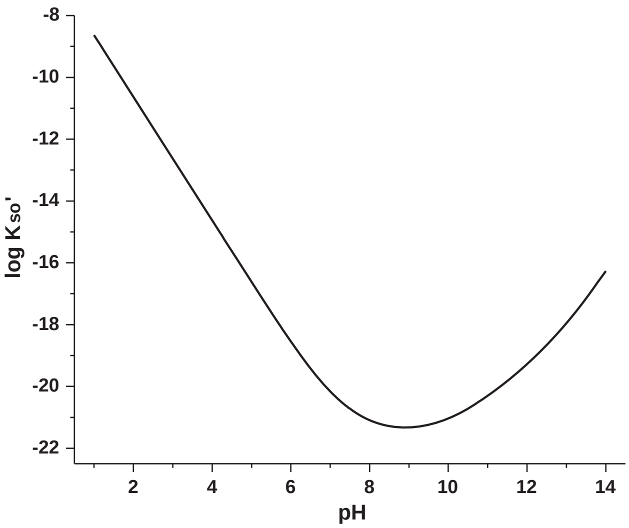

Fig. 1. Conditional solubility products constant at various pH taking into account side reactions coefficients of Pb^{2+} and S^{2-}.

A predominant side reaction in our experiments is due to pH effect. This is shown by plotting conditional solubility of lead sulfide as shown in Fig. 1. Minimum solubility of lead sulfide is obtained in the pH range 8–10. In this region the interfering effect of hydrogen ions with sulfide and hydroxide ions with lead are quite small and only 10^{-10} to $10^{-10.5}$ M PbS are dissolved. Lead sulfide undergoes pH dependent reduction/oxidation reactions that can change the analytical concentration of Pb^{2+}. The electrical potential-pH (Pourbaix) diagram for the Pb–S–$\mathrm{H_2O}$ system (Fig. 2) helps to illustrate possible redox effects [31]. For this reason the lines corresponding to lead activity in the solution of 10^{-1} and 10^{-9} mol dm^{-3}, are marked in the diagram. From Pourbaix diagram it can be seen that the shift in the potential values (versus NHE) under which the lead sulfide oxidizes is strictly connected to the concentration of lead in the solution. Less concentrated solution of lead promotes oxidation at lower potential values, the fact well known for sparingly soluble sulfides [32]. In our case of investigation the operative potential values are from −0.38 V to −0.18 V (taken from Fig. 2 and recalculated for the NHE) and the pH range unbuffered solutions was 4 < pH < 7, indicated by arrow in Fig. 4. The oxidative dissolution of lead sulfide results in formation of soluble sulfates coupled with increased lead ion concentration at the membrane surface, according to the

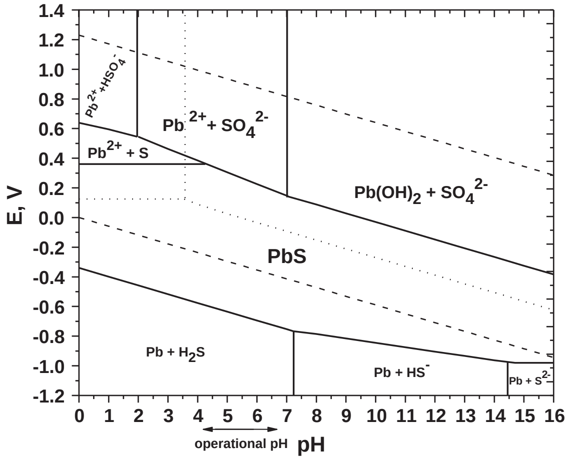

Fig. 2. E–pH diagram of Pb–S–$\mathrm{H_2O}$ system at 25 °C. (—) $[\mathrm{Pb}^{2+}] = 10^{-1}$ mol dm^{-3}, $[\mathrm{HSO_4}^-] = [\mathrm{SO_4}^{2-}] = [\mathrm{H_2S}] = [\mathrm{HS}^-] = [\mathrm{S}^{2-}] = 10^{-1}$ mol dm^{-3}. (···) $[\mathrm{Pb}^{2+}] = 10^{-9}$ mol dm^{-3}, $[\mathrm{HSO_4}^-] = [\mathrm{SO_4}^{2-}] = [\mathrm{H_2S}] = [\mathrm{HS}^-] = [\mathrm{S}^{2-}] = 10^{-1}$ mol dm^{-3}. (- - -) Potential stability window for water at 25 °C. The arrow shows pH range in unbuffered solutions.

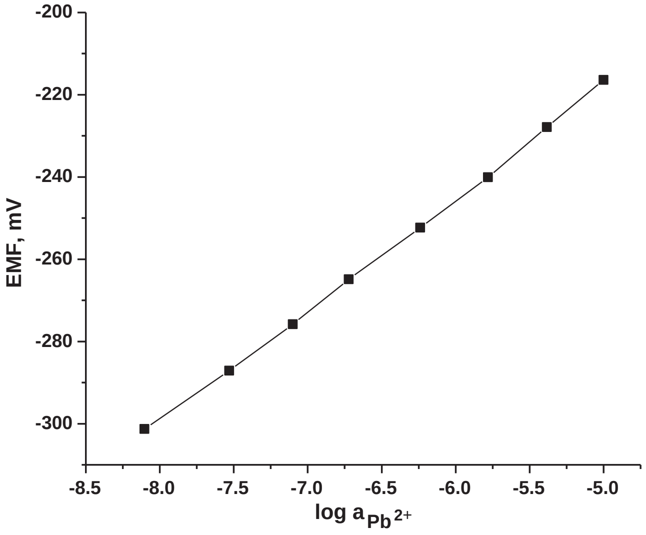

Fig. 3. Calibration curve of $\mathrm{Pb^{2+}}$-ISE obtained from titration of $\mathrm{Pb^{2+}}$ in Tris buffer, pH 8 with Tiron.

reaction:

$$\mathrm{PbS} + 4\mathrm{H_2O} \rightarrow \mathrm{Pb^{2+}} + \mathrm{SO_4^{2-}} + 8\mathrm{H^+} + 8\mathrm{e^-} \qquad (7)$$

Above process is reflected by the apparent deterioration of detection limit, which is described by the contribution $\beta - \alpha > 0$ in the Eq. (1).

In view of Figs. 1 and 2 to minimize the influence of parasitic effects we found advantageous to remove oxygen (e.g. by purging argon) and/or to decrease redox potential of the solutions without affecting concentrations of free lead ion (e.g. by addition of small amounts, less than 2 mg $\mathrm{dcm^{-3}}$, of ascorbic acid) [4,7]. Additionally, we found that an extrathermodynamic factor, i.e. mixing, brings favorable effects. However, we did not dedicate a special study, except of a very practical selector: with or without mixing. Obviously, mixing enhanced transport and facilitated removal of reactants from/to the solid membrane as well as removal of dissolved oxygen by purging sample solution with argon.

4. Results and discussions

4.1. Metal titration method

Metal titration is an excellent way to get information about the performance of ISEs at low concentrations [16]. Free lead ion activities were calculated after every addition of Tiron from the pH values recorded during the titration and total concentration of complexing agent added to the solution of lead nitrate. The protonation constants used in the calculations are: $\log K_{\mathrm{HL}}^{\mathrm{H,L}} = 12.7$ and $\log K_{\mathrm{H_2L}}^{\mathrm{HL,H}} = 7.7$ for $\mathrm{H_2}$Tiron, and the stability constants $\log K_{\mathrm{PbL}}^{\mathrm{Pb,L}} = 11.95$, $\log K_{\mathrm{PbL_2}}^{\mathrm{Pb,L}} = 6.35$ [26]. The results of the metal titration method are presented in Fig. 3. In this experiment the solid-state electrode exhibits a linear response in the low range of lead activity, from 10^{-5} to $10^{-8.1}$ mol $\mathrm{dm^{-3}}$. The slope of the calibration line in the entire activity range is 27.8 mV/dec. Use of Tiron as a complexing agent allowed to obtain linearity of the calibration line down to $p\mathrm{Pb^{2+}} = 8.1$. This shows that by minimizing interferences the solid-state lead-selective electrode is closer to the theoretical value of the low detection limit indicated by the solubility product of lead sulfide ($-\log S = 13.3$, see Table 1). However, in this method the free activity of $\mathrm{Pb^{2+}}$ is supported by relatively high total concentration of this ion, so as in the case of ionic buffers its analytical value is rather limited.

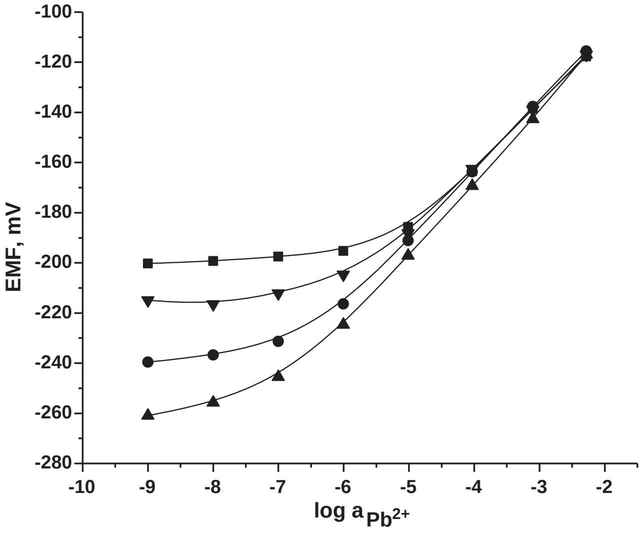

Fig. 4. Influence of stirring and purging the unbuffered solution with argon on lowering the detection limit of the $\mathrm{Pb^{2+}}$-ISE: (■) calibration without stirring and purging argon, (▼) purging argon, (•) stirring, (▲) purging argon while stirring.

4.2. Direct calibration method

The potentiometric behavior of a $\mathrm{Pb^{2+}}$ solid-state membrane ISE in the unbuffered solutions of the main ion is shown in Fig. 4. By investigating various conditions of the calibration procedure it was found that stirring and purging the sample solution with argon exert influence on the performance of the electrode. The slope calculated from the linear part of the calibration curve for all applied conditions was close to Nernstian. As expected, the lowest detection limit was obtained for calibration when purging with argon and solution stirring were applied, and was $10^{-7.1}$ mol $\mathrm{dm^{-3}}$ with a slope of 28.9 mV/dec. In comparison with the calibration without stirring and purging argon the detection limit was lowered by about two orders of magnitude.

4.3. Kinetic calibration method

The concept of kinetic calibration takes advantage of concentration-dependent potential changes over time after the same pretreatment of the Pb-ISE membranes made by polishing, titration with sodium sulfide and subsequent soaking in

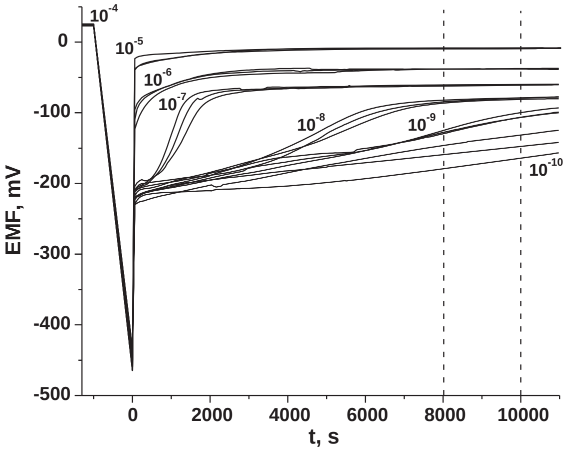

Fig. 5. Kinetic curves recorded for the $\mathrm{Pb^{2+}}$-ISE at different lead ion activities. The dashed lines show the time interval where data was collected for the slope calculation.

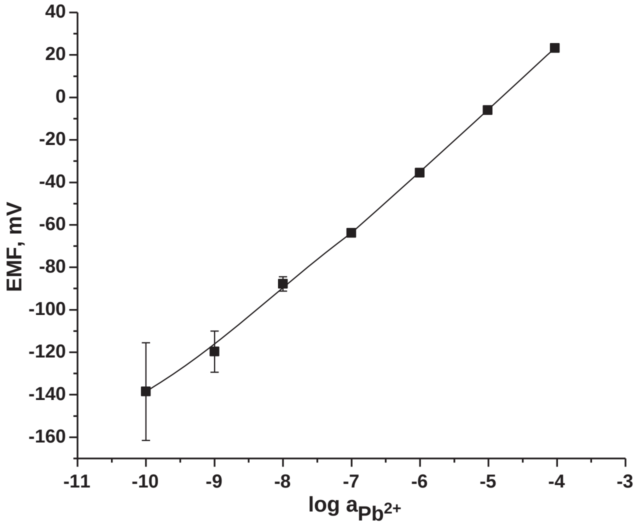

Fig. 6. Calibration curve of Pb^{2+}-ISE obtained from the kinetic calibration procedure. The error bars show the standard deviation for three measurements.

sodium sulfide. The kinetic curves of the investigated activities of the lead ion are presented in Fig. 5. Each time the solid-state membrane electrode was bathed in the solution with extremely low Pb^{2+} activities, owing to above described titration procedure. Subsequently, placing the electrodes in the calibrating solutions kinetic curves were recorded. The concentrations of lead (II) in the most diluted solutions were checked by ICP-MS. For 10^{-9} and 10^{-10} mol dm^{-3} of lead (II) nitrate the lead concentrations measured by ICP-MS were $10^{-9.01}$ and $10^{-10.1}$ mol dm^{-3}, respectively. It was observed that the kinetic curves recorded in higher activity of lead ion (10^{-5}, 10^{-6} mol dm^{-3} Pb^{2+}) were reaching stable potential after a short time while the kinetic curves recorded in diluted solutions (in the range 10^{-9} to 10^{-10} mol dm^{-3} Pb^{2+}) indicate that a stable potential (drift less than 0.02 mV/min) was not attained. Nevertheless, from the range from 8000 to 10 000 s a clear distinction between each curve for the particular concentration was observed. This effect can be attributed to concentration and time dependent adsorption [4]. Averaging the potential values (arithmetical mean) from the range of 8000–10 000 s for three consecutive kinetic curves of each activity of Pb^{2+} the calibration curve presented in Fig. 6 was obtained. The calibration curve is plotted with marked standard deviation. The sensitivity was observed in a broad range of lead activity with close to Nernstian slope of 29.3 mV/dec and the detection limit $10^{-9.0}$ mol dm^{-3}.

5. Conclusions

Although recent research concentrates on plastic membranes, the solid state ISE offer advantage of simplicity that was overlooked. By optimizing the conditions in the solutions, i.e. minimizing side reactions and parasitic processes, and by use of a procedure of cleaning the membrane and introducing optimized readout times (kinetic method) we are able to extend the linear measurement range for the solid-membrane lead ISE in unbuffered solutions down to $10^{-9.0}$ mol dm^{-3}. This is still far from the possibility that is ideally offered by the thermodynamic solubility of PbS. However, from a practical point of view, and in comparison to heavily advertised possibilities obtained with plastic-based Pb^{2+} ISEs, this is an attractive opportunity. It is shown that by applying simple changes in the calibration procedure the low detection limit in the case of a solid-membrane ISE may be lowered by two orders of magnitude.

We believe that by this report we open a new important avenue for the direct electrochemical measurement of ions in nanomolar range by using solid-state membrane electrodes.

Acknowledgements

The authors acknowledge the Graduate School of Chemical Sensors and Microanalytical Systems (CHEMSEM) and MATERA ERA-NET EU TEKES (2084/31/06) project (MASTRA) for the financial support.

References

[1] J. Bobacka, A. Ivaska, A. Lewenstam, Chem. Rev. 108 (2) (2008) 329.
[2] W.E. Morf, G. Kahr, W. Simon, Anal. Chem. 46 (11) (1974) 1538.
[3] A. Hulanicki, A. Lewenstam, Talanta 23 (9) (1976) 661.
[4] A. Hulanicki, A. Lewenstam, M. Maj-Zurawska, Anal. Chim. Acta 107 (1979) 121.
[5] E. Pretsch, Trends Anal. Chem. 26 (2007) 46.
[6] T. Sokalski, A. Ceresa, T. Zwickl, E. Pretsch, J. Am. Chem. Soc. 119 (1997) 11347.
[7] J. Kontoyannakos, G.J. Moody, J.D.R. Thomas, Anal. Chem. Acta 85 (1976) 46.
[8] R.P. Buck, Anal. Chem. 40 (10) (1968) 1432.
[9] D.J. Crombie, G.J. Moody, J.D.R. Thomas, Anal. Chem. Acta 80 (1975) 1.
[10] Yu. G. Vlasov, E.A. Bychkov, A.V. Legin, Sens. Actuators B 10 (1992) 55.
[11] R.W. Burnett, A.K. Convington, N. Fogh-Andersen, W.R. Külpmann, A. Lewenstam, A.H. Maas, O. Müller-Plathe, A.L. VanKessel, W.G. Zijlstra, Clin. Chem. Lab Med. (2000).
[12] K. Cammann, Das Arbeiten mit Ionenselektiven Elektroden, Springer-Verlag, Berlin, Heidelberg, 1973.
[13] E.H. Hansen, C.G. Lamm, J. Růžička, Anal. Chim. Acta 59 (1972) 403.
[14] A. Ringbom, L. Harju, Anal. Chim. Acta 59 (1972) 3347.
[15] A. Hulanicki, T. Sokalski, A. Lewenstam, Microchim. Acta 3 (1–6) (1988) 119.
[16] A. Hulanicki, T. Krawczynski, A. Lewenstam, Anal. Chim. Acta 158 (1984) 343.
[17] A. Lewenstam, T. Sokalski, A. Hulanicki, Talanta 32 (7) (1985) 531.
[18] E.W. Baumann, Anal. Chim. Acta 54 (1971) 189.
[19] M. Trojanowicz, Talanta 26 (10) (1979) 985.
[20] E. Pungor, E. Schmidt, K. Toth, Proc. IMEKO (1968) 121.
[21] J.F. Lechner, I. Sekerka, J. Electroanal. Chem. 57 (1974) 317.
[22] A. Hulanicki, R. Lewandowski, A. Lewenstam, Anal. Chim. Acta 110 (1979) 97.
[23] N. Parthasarathy, J. Buffle, D. Monnier, Anal. Chim. Acta 68 (1974) 185.
[24] J. Buffle, N. Parthasarathy, W. Haerdi, Anal. Chem. Acta 68 (1974) 253.
[25] J. Buffle, N. Parthasarathy, Anal. Chim. Acta 93 (1977) 111.
[26] J. Inczédy, Analytical Applications of Complex Equilibria, John Wiley & Sons Limited, Baffins Lane, Chichester, Sussex, England, 1976.
[27] R.C. Weast, M.J. Astle, W.H. Beyer, CRC Handbook of Chemistry and Physics, 67th edition, CRC Press, Inc, Boca Raton, Florida, 1986.
[28] T. Sokalski, W. Kucza, M. Danielewski, A. Lewenstam, Anal. Chem. 81 (2009) 5016.
[29] J. Růžička, C.G. Lamm, Anal. Chim. Acta 54 (1971) 1.
[30] A. Ringbom, Complexation in Analytical Chemistry, Wiley-Interscience, New York, 1963.
[31] A. Lewenstam, A. Hulanicki, E. Ghali, in: A. Ivaska, A. Lewenstam, R. Sara (Eds.), Contemporary Electroanalytical Chemistry, Plenum Press, New York and London, 1988, pp. 213–222.
[32] E. Ghali, B. Dandapani, A. Lewenstam, J. Appl. Electrochem. 12 (1982) 367.